Invited - Sub-Wavelength Focusing in Loaded Transmission Line Negative Refractive Index Metamaterials

(Invited Paper)

Ashwin K. Iyer, Anthony Grbic, and George V. Eleftheriades

The Edward S. Rogers Sr. Dept. of ECE, University of Toronto, Ontario, M5S 3G4, CANADA

Abstract — We have previously demonstrated that a new class of planar Negative Refractive Index Metamaterials (NRIMs) can be constructed by periodically loading a host transmission line medium with inductors and capacitors in a dual (high-pass) configuration, and we have experimentally demonstrated focusing of a cylindrical wave inside such a NRIM, using a single-interface prototype. In this paper, we examine the conditions required to observe sub-wavelength focusing using a theory based on the plane-wave expansion of cylindrical waves, supplemented by permeability and permittivity functions characteristic to our NRIMs. This theory is validated by full-wave simulations and experimental data for a single-interface structure, and subsequently applied to the study of a two-interface (NRIM slab lens) structure. Finally, we present microwave circuit simulations showing clear, sub-wavelength focusing in a realizable NRIM lens.

I. INTRODUCTION

In the late 1960s, V. G. Veselago proposed that materials exhibiting simultaneously negative permeability and permittivity would also exhibit a negative refractive index [1]. These Negative Refractive Index Metamaterials (NRIMs), also referred to as Left-Handed Media (LHM), presented a host of interesting features, including focusing using flat lenses, and the reversal of both Cherenkov radiation and the Doppler shift. Artificial materials displaying these properties were first realized at UCSD in 1999 [2] following the development of Pendry's Split-Ring-Resonator (SRR) [3]. Pendry also discovered that NRI lenses enhance evanescent waves, and can therefore restore sub-wavelength features at the focal plane, essentially overcoming the diffraction limit [4].

A different class of NRIMs was introduced last year in this conference by Iyer and Eleftheriades, based on the reactive loading of a 2-D transmission line (TL) host medium [5]. Specifically, these planar, broadband NRIMs consist of a 2-D transmission line grid, periodically loaded with capacitors and inductors in a dual (high-pass) configuration. Focusing by means of the negative index property was verified experimentally using a prototype consisting of a microstrip-line based NRIM interfaced with a Positive Refractive Index (PRI) TL medium. These
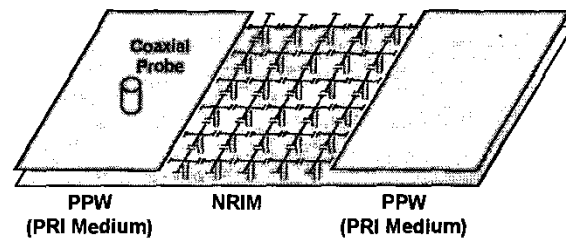

Figure 1: Two-interface PPW-NRIM-PPW structure

experimental results were presented in [5] and subsequently documented in [6]. A CPW implementation was also used to experimentally verify leaky backward radiation from the fundamental spatial harmonic, analogous to Veselago's reversed Cherenkov radiation [7–8].

This paper extends the discussion of the single-interface structure to a two-interface structure consisting of a transmission line-based NRIM slab inserted between two PRI media, as depicted in Figure 1. Practically, the NRIM is constructed by loading a 2-D grid of microstrip lines with surface-mounted chip capacitors in series and chip inductors in shunt embedded into the substrate. The PRI media are provided by two parallel-plate waveguides (PPWs), one of which is excited using a vertical coaxial probe as shown in Figure 1. This paper shall examine the conditions required to observe sub-wavelength focusing in such a two-interface structure. A theory based on the plane-wave expansion of cylindrical waves is employed, and supplemented by permeability and permittivity expressions characteristic to periodically loaded transmission line NRIMs [6,8]. The theory is first validated by supporting full-wave simulation and experimental data for the single-interface lens device, and subsequently applied to the two-interface case. Finally, microwave circuit simulation data showing sub-wavelength focusing using a transmission line NRIM slab lens are presented.
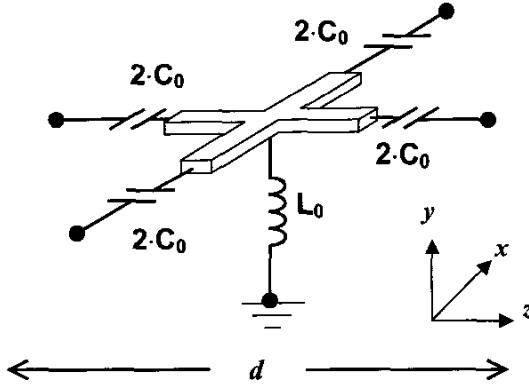
Figure 2: Unit cell for the 2-D transmission line NRIM.

Figure 3: Two-interface NRIM slab lens structure. The arrows depict the wavevectors in each medium.

II. THEORY

The physical properties of conventional dielectrics can be artificially synthesized in the long-wavelength regime using periodic L-C networks in a low-pass configuration, for which the series inductance and shunt capacitance yield the material permeability and permittivity, respectively. In the dual configuration, these structures yield simultaneously negative material parameters, forming the basis for the introduction of transmission line NRIMs [5]. This is illustrated by considering the unit cell for the periodic, 2-D NRIM structure, shown in Figure 2. When the unit cell dimension d is much smaller than a wavelength, the medium may be viewed as homogeneous. The predominance of a TM$_y$ mode in these structures justifies the equivalent material parameters,

$$\mu_L = \mu_R - \frac{1}{\omega^2 C_0 d}, \quad \varepsilon_L = \varepsilon_R - \frac{1}{\omega^2 L_0 d}, \tag{1}$$

where μ_R and ε_R describe the host transmission line medium. These expressions are characteristic to transmission line NRIMs [6,8], and demonstrate that the equivalent material parameters may be made simultaneously negative.

The arrangement presently studied is depicted in Figure 3. For generality, we permit the RHM M1 and M2 to possess different permittivities and permeabilities (μ_1, ε_1 and μ_2, ε_2, respectively), thereby introducing the possibility of reflections. The NRIM slab of thickness $2 \cdot d_L$ is placed at $x=d_R$ and excited by a vertical (y-directed) line source located at $x=z=0$. The plane-wave expansion method is then used to solve the problem of Figure 3. This method has been previously employed by Kong et al. [9] to describe the refraction of a Gaussian beam through a medium with negative material parameters; here, we apply
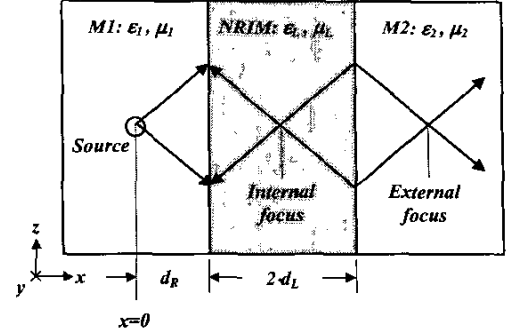
it to transmission line NRIMs exclusively to describe their ability to focus cylindrical waves (i.e. derive the Green's function). The fields in each medium $i=\{1,L,2\}$ are represented as follows:

$$E_{y,i}(x,z) = \frac{1}{2\pi} \int_{-\infty}^{\infty} \tilde{E}_{y,i}(x,k_{x,i}) e^{-jk_{z,i}z} dk_{z,i}, \tag{2}$$

$$k_{x,i} = \pm j\sqrt{k_{z,i}^2 - k_i^2}, \quad k_i^2 = \omega^2 \varepsilon_i \mu_i. \tag{3}$$

Equation (3) describes the dispersion of material i, and the positive root is chosen only for the NRIM. The resulting expression for the spectral components of the y-directed electric field in M2 is

$$\tilde{E}_{y,2} = \tilde{E}_{y,1}\Big|_{x=0} \left\{ \frac{4\tau_B e^{-jk_{x,1}d_R} e^{-jk_{x,2}(x-(d_R+2d_L))}}{(\tau_A+1)(\tau_B+1)e^{2jk_{x,L}d_L} - (\tau_A-1)(\tau_B-1)e^{-2jk_{x,L}d_L}} \right\} \tag{4}$$

where

$$\tau_A = \frac{k_{x,L}\mu_1}{k_{x,1}\mu_L}, \quad \tau_B = \frac{k_{x,L}\mu_2}{k_{x,2}\mu_L}, \quad \tilde{E}_{y,1}\Big|_{x=0} = -\frac{\omega\mu_1}{2k_{x,1}}. \tag{5}$$

The coefficient outside the parentheses of (4) is the spectral representation of the source at $x=0$. When the impedances of the media are perfectly matched and the relative refractive index $n_{REL} = -1$ ($k_{x,1} = k_{x,2} = -k_{x,L}$, $\mu_1 = \mu_2 = -\mu_L \Rightarrow \tau_A = \tau_B = 1$), equation (4) reduces to

$$\tilde{E}_{y,2} = \tilde{E}_{y,1}\Big|_{x=0} e^{-jk_{x,1}(x-4d_L)}, \tag{6}$$

from which it is clear that the source spectrum originating in M1 is identically recovered at the image plane in M2, a distance of $4 \cdot d_L$ from the source. Symmetry arguments further require that $d_R=d_L$, implying that the source and image are equidistant from their nearest interfaces. Since the infinitesimal source and its image are identical, the term 'sub-wavelength focusing' is justified.

200

III. Results

A. Single-Interface Structure

The focusing phenomenon inherent to NRIMs was verified in experiment using a single-interface, transmission line-based NRIM prototype, in which a 55mm×50mm parallel-plate waveguide, interfaced with a 55mm×30mm NRIM and excited using a vertical probe, produced a focal spot inside the NRIM that persisted and varied characteristically over an octave bandwidth [5–6]. The results were correlated with Method-of-Moments full-wave simulations of the same structure, and showed good correspondence of the normalized field distributions over the focal region. Here, these results are correlated with those predicted by the plane wave expansion theory presented in this paper. Specifically, the vertical (y-directed) electric fields are computed in the NRIM region at 1.5GHz using (1) – (5). These results are presented in Figure 4 along with full-wave simulation and experimental results.

RHM   **LHM**

Full-Wave Field Simulation   **Experiment**   **Theory**
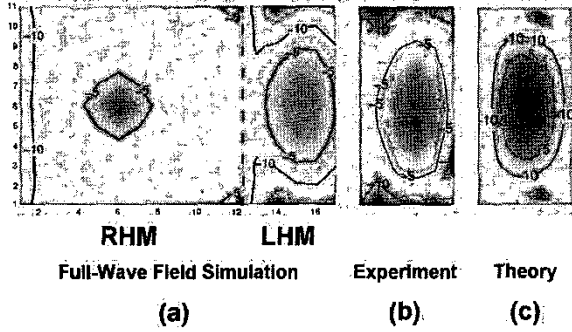
(a)   **(b)**   **(c)**

Figure 4: Correspondence of (a) MoM full-wave field simulation, (b) experimental data, and (c) results of plane wave expansion analysis at 1.5 GHz (normalized to the maximum respective field transmission in each case).

Experiments were also performed on a larger single-interface structure featuring a 100mm×200mm NRIM region. The normalized fields at the focal plane, determined experimentally and predicted by the plane wave expansion theory at 1.8GHz, are presented in Figure 5. The correspondence is evident.

B. Two-Interface Structure

It has been mentioned that an exact recreation of the source at the image plane described by (6) can be achieved only under (i) wave impedance-matched conditions (7a), (ii) when n_{REL} at both interfaces is identically -1 (7b), and
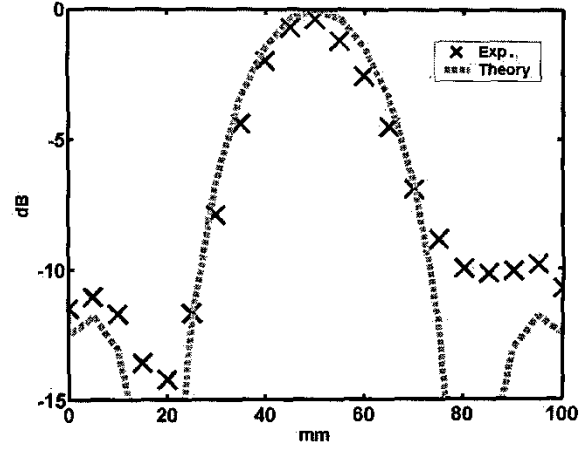

Figure 5: Focal plane of 100mm×200mm transmission line NRIM at 1.8GHz (normalized experimental data and plane-wave expansion analysis).

(iii) when the integration includes all spatial frequency components, including the evanescent waves.

$$\sqrt{\frac{\mu_L(\omega)}{\varepsilon_L(\omega)}} = \sqrt{\frac{\mu_R}{\varepsilon_R}} \qquad (7a)$$

$$\sqrt{\mu_L(\omega)\varepsilon_L(\omega)} = \sqrt{\mu_R\varepsilon_R} \qquad (7b)$$

To examine the first condition, we note that substituting (1) into (7a) results in the following equality:

$$\frac{L_0}{C_0} = \frac{\mu_R}{\varepsilon_R}. \qquad (8)$$

The reader will note that this result (i.e., equation (8)), describing the paraxial matching of the wave impedances, is invariant to frequency. The index of refraction, however, is necessarily frequency dependent due to the dispersive nature of the material parameters of (1). Consequently, the second condition described by (7b) can only be satisfied at a particular frequency ω_0, given by

$$\omega_0^2 = \left(L_0 \cdot \varepsilon_R d + C_0 \cdot \mu_R d\right)^{-1}. \qquad (9)$$

Equations (8) and (9) jointly specify the appropriate loading parameters, for which (7a) and (7b) are simultaneously satisfied:

$$L_0 = \frac{1}{2\omega_0^2\varepsilon_R d}, \quad C_0 = \frac{1}{2\omega_0^2\mu_R d}. \qquad (10)$$

Equation (1) may now be represented as

$$\mu_L = \mu_R\left\{1 - 2\left(\omega_0/\omega\right)^2\right\}, \quad \varepsilon_L = \varepsilon_R\left\{1 - 2\left(\omega_0/\omega\right)^2\right\}. \qquad (11)$$

Equation (11) reveals that $\mu_L/\mu_R = \varepsilon_L/\varepsilon_R = n_{REL} = -1$ at $\omega = \omega_0$. In this case, the source (at $x=0$) is perfectly focused at the image plane (at $x=4 \cdot d_R$), as shown in Figure 6a for $\omega = \omega_0 = 2\pi \times 1.0$GHz. Furthermore, there are no reflections, since $n_{REL} = -1$ makes all angles effectively paraxial [6]. The sensitivity of the requirement $n_{REL} = -1$ for sub-wavelength focusing can be demonstrated simply by detuning the operating frequency away from ω_0. As an example, a shift from $\omega_0 = 2\pi \times 1.0$GHz to $\omega = 2\pi \times 1.05$GHz results in $\mu_L/\mu_R = \varepsilon_L/\varepsilon_R = n_{REL} = -0.8141$. In this case, the source and image appear as shown in Figure 6b, and it is immediately apparent that both the transmission and the sharpness of the image are degraded at the image plane. Furthermore, $n_{REL} \neq -1$ implies that the wave impedances are mismatched away from the principal axis, resulting in reflections apparent at the source plane.

To examine the third condition, it should be noted from (2) and (3) that the spatial frequency region $|k_{z,i}| > |k_i|$ contains evanescent components that, in conventional media, decay exponentially in x (see Figure 3). It has been shown by Pendry that these components are actually enhanced in NRIMs, and contribute significantly to the restoration of the sub-wavelength features of the source at the image plane [4]. Figure 6c depicts the vertical electric fields at the source plane and at the image plane with $n_{REL} = -1$ (the magnitude of the wavevectors $|k_i|$ in the individual media become equal), but with varying ranges of integration. These results confirm that the enhancement of the evanescent portion of the spectrum in the NRIM plays a significant role in reconstructing the sharper features of the source at the image plane, as predicted by Pendry [4].

Lastly, the finite two-interface structure of Figure 3 was implemented using the Agilent-ADS microwave circuit simulator, and designed with $n_{REL} = -1$ at $\omega_0 = 2\pi \times 1.0$GHz. The voltages at the source and image planes are presented in Figure 6d, showing perfect recreation of the source and hence, clear sub-wavelength focusing by a realizable NRIM lens.

IV. CONCLUSION

We have examined the conditions required to observe sub-wavelength focusing using a transmission line NRIM slab. The analysis, based on the plane wave expansion of cylindrical waves, has been validated by microwave circuit and full-wave field simulations, as well as experimental results for both small and large NRIM lenses. Clear sub-wavelength focusing results were presented using Agilent-ADS simulations.
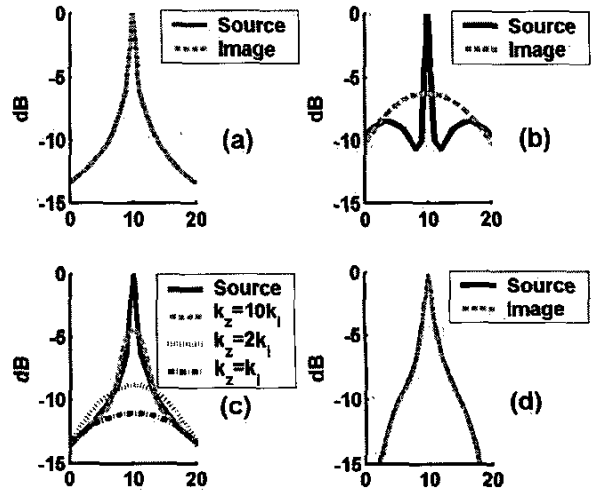

Figure 6: (a) Source and image planes for $n_{REL} = -1$; (b) source and image planes for $n_{REL} = -0.8141$; (c) contribution of evanescent components to recreation of source at image plane; (d) microwave circuit simulations showing perfect focusing of the source at the image plane. The horizontal axes are labeled according to cell number.

REFERENCES

[1] V. G. Veselago, "The electrodynamics of substances with simultaneously negative values of ε and μ," *Sov. Phys. Usp*, vol. 10, no. 4, pp. 509-514, Jan.-Feb.1968.

[2] R. A. Shelby, D. R. Smith, S. Schultz, "Experimental verification of a negative index of refraction," *Science*, vol. 292, 6 April 2001, pp. 77-79.

[3] J. B. Pendry, A. J. Holden, D. J. Robins, W. J. Stewart, "Magnetism from conductors and enhanced nonlinear phenomena," *IEEE Trans. on Microwave Theory and Tech.*, vol. 47, no. 11, pp. 2075-2084, Nov. 1999.

[4] J. B. Pendry, "Negative refraction makes a perfect lens," *Phys. Rev. Lett.*, vol. 85, no. 18, pp. 3966-3969, Oct. 2000.

[5] A. K. Iyer and G. V. Eleftheriades, "Negative refractive index metamaterials supporting 2-D waves," in *IEEE MTT-S Int. Microwave Symp. Dig.*, vol. 2, Seattle, WA, June 2-7, 2002, pp. 1067-1070.

[6] G. V. Eleftheriades, A. K. Iyer, P. C. Kremer, "Planar negative refractive index media using periodically L-C loaded transmission lines," *IEEE Trans. on Microwave Theory and Tech.*, vol. 50, no. 12, pp. 2702-2712, Dec. 2002.

[7] A. Grbic, G. V. Eleftheriades, "A backward-wave antenna based on negative refractive index L-C networks," in *IEEE Int. Symp. Ant. and Propag.*, vol. 4, San Antonio, TX, June 16-21, 2002, pp. 340-343.

[8] A. Grbic, G. V. Eleftheriades, "Experimental verification of backward-wave radiation from a negative refractive index metamaterial," *Journal of Appl. Phys.*, vol. 92, no. 10, pp. 5930-5935, November 2002.

[9] J. A. Kong, B. Wu, Y. Zhang, "Lateral displacement of a Gaussian beam reflected from a grounded slab with negative permittivity and permeability," *Appl. Phys. Lett.*, vol. 80, no. 12, pp. 2084-2086, March 2002.